Society For Biomaterials

Fabrication and *in vivo* thrombogenicity testing of nitric oxide generating artificial lungs

Kagya A. Amoako,[1,2] Patrick J. Montoya,[3] Terry C. Major,[1] Ahmed B. Suhaib,[1] Hitesh Handa,[1] David O. Brant,[1] Mark E. Meyerhoff,[4] Robert H. Bartlett,[1] Keith E. Cook[1,5]

[1]Departments of Surgery, University of Michigan Medical Center,
1150 W Medical Center Drive B560B MSRBII, Ann Arbor, MI 48109-0686
[2]Department of Internal Medicine, Cardiology, University of Michigan Medical Center
[3]Medarray Inc., Ann Arbor, MI
[4]Department of Chemistry, University of Michigan, Ann Arbor, MI
[5]Department of Biomedical Engineering, University of Michigan, Ann Arbor, MI 48109-0686

Received 11 June 2012; revised 16 January 2013; accepted 4 February 2013
Published online 24 April 2013 in Wiley Online Library (wileyonlinelibrary.com). DOI: 10.1002/jbm.a.34655

Abstract: Hollow fiber artificial lungs are increasingly being used for long-term applications. However, clot formation limits their use to 1–2 weeks. This study investigated the effect of nitric oxide generating (NOgen) hollow fibers on artificial lung thrombogenicity. Silicone hollow fibers were fabricated to incorporate 50 nm copper particles as a catalyst for NO generation from the blood. Fibers with and without (control) these particles were incorporated into artificial lungs with a 0.1 m^2 surface area and inserted in circuits coated tip-to-tip with the NOgen material. Circuits ($N = 5$/each) were attached to rabbits in a pumpless, arterio-venous configuration and run for 4 h at an activated clotting time of 350–400 s. Three control circuits clotted completely, while none of the NOgen circuits failed. Accordingly, blood flows were significantly higher in the NOgen group (95.9 $\pm$ 11.7, $p < 0.01$) compared to the controls (35.2 $\pm$ 19.7; mL/min), and resistance was significantly higher in the control group after 4 h (15.38 $\pm$ 9.65, $p < 0.001$) than in NOgen (0.09 $\pm$ 0.03; mmHg/mL/min). On the other hand, platelet counts and plasma fibrinogen concentration expressed as percent of baseline in control group (63.7 $\pm$ 5.7%, 77.2 $\pm$ 5.6%; $p < 0.05$) were greater than those in the NOgen group (60.4 $\pm$ 5.1%, 63.2 $\pm$ 3.7%). Plasma copper levels in the NOgen group were 2.8 times baseline at 4 h (132.8 $\pm$ 4.5 μg/dL) and unchanged in the controls. This study demonstrates that NO generating gas exchange fibers could be a potentially effective way to control coagulation inside artificial lungs. © 2013 Wiley Periodicals, Inc. J Biomed Mater Res Part A: 101A: 3511–3519, 2013.

Key Words: artificial lung, nitric oxide, extracorporeal circulation, silicone, thrombosis, biocompatibility

How to cite this article: Amoako KA, Montoya PJ, Major TC, Suhaib AB, Handa H, Brant DO, Meyerhoff ME, Bartlett RH, Cook KE. 2013. Fabrication and *in vivo* thrombogenicity testing of nitric oxide generating artificial lungs. J Biomed Mater Res Part A 2013:101A:3511–3519.

INTRODUCTION

Hollow fiber artificial lungs are increasingly being used for long-term applications. These applications include extracorporeal membrane oxygenation, pumpless arterio-venous carbon dioxide removal, and thoracic artificial lungs. However, thrombosis often limits the longevity of extracorporeal membranes. Blood contact leads to clot formation, increased resistance, and decreased gas exchange efficiency.[1–4] Furthermore, shed thromboemboli from these devices can cause organ dysfunction. Antithrombotic coatings for blood-contacting surfaces including membrane lungs are available,[5–10] but these coatings have not worked well enough to markedly reduce clot formation or eliminate the need for systemic anticoagulation.

One possible solution to this problem is the use of NO flux from the surfaces of the artificial lung. Nitric oxide (NO) is a short-acting, potent platelet inhibitor that is normally produced by endothelial cells.[11] The half-life of NO is only 2–5 s in blood.[12] As a result, NO delivery from polymer surfaces has been examined as a means to focus anticoagulation solely at the biomaterial surface without systemic effects or cell damage.[13] Accordingly, previous studies have shown that platelet adhesion is reduced on polymers that either release stored NO or generate it from NO donors in blood if the NO flux exceeds that of the endothelium.[14,15]

The goal of this study was to examine the effect of NO generating (NOgen) surfaces in artificial lungs for the first time. Silicone (polydimethylsiloxane) gas exchange fibers were thus manufactured to incorporate Cu particles. The Cu particles catalyze NO formation in blood via decomposition of circulating *s*-nitrosothiols via the mechanism in Figure 1A.[16–18] NO generation and clotting have both been shown

Correspondence to: K. E. Cook; e-mail: keicook@umich.edu; K. A. Amoako; e-mail: kagyaa@umich.edu
Contract grant sponsor: National Institutes of Health; contract grant number: 2R01 HI069420-06

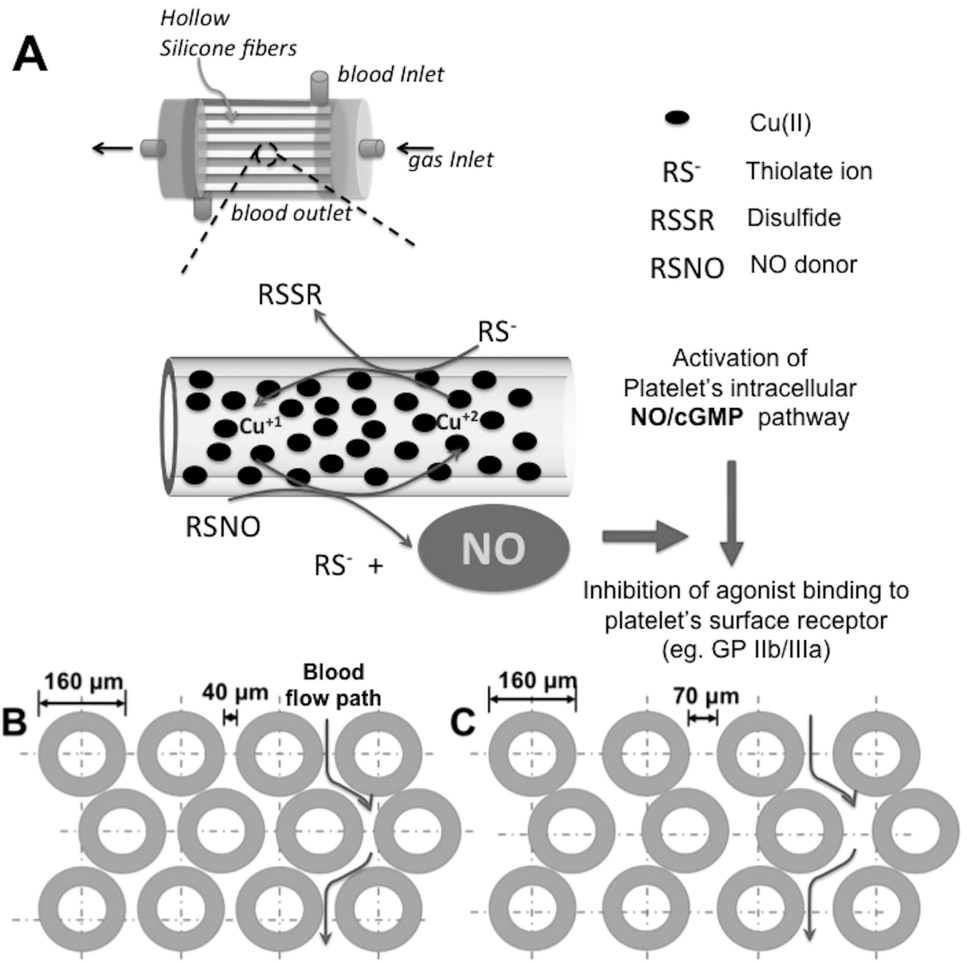

FIGURE 1. (A) A model of Cu-mediated NO generation from circulating S-nitrosothiols by hollow fiber membrane lungs for platelet inhibition, (B) the linear fiber spacing of NOgen lungs, and (C) that of commercial lungs.

to be linearly related to surface expression of Cu.[19] These fibers were incorporated in miniature artificial lungs, which were inserted into a circuit that was similarly coated tip-to-tip with the NOgen material. The circuit was then evaluated for thrombogenicity for a period of 4 h in a pumpless arterio-venous circulation model in rabbits.

MATERIALS AND METHODS

Circuit components

Radial flow artificial lungs were constructed with NOgen or pure silicone hollow fibers [Fig. 2(A)]. Both fiber types were constructed at Medarray, Inc (Ann Arbor, MI) using a proprietary two-part silicone formulation (MedArray Inc, Ann Arbor MI). NOgen fibers were doped with 10 wt% of 50 nm Cu particles (Sigma Aldrich, St. Louis, MO). The hollow fibers had an average inner and outer diameter of 100 and 160 μm. Each fiber bundle had a path length, axial length, and void fraction of 1.1 ± 0.2 cm, 2.7 ± 0.5 cm, and 0.37 respectively. The prime volume and surface area were 20 mL and 0.09 m^2. To examine the non-thrombogenicity of NO generating artificial lungs in short-term experiments, a dense, aggressive artificial lung design is required to accelerate clot formation. The fiber bundle's void fraction was thus 33% compared to a typical value of 50% in a commercial oxygenator. Void fraction is defined as 1-(solid space/total space), where solid space is the volume occupied by fiber material and total space is the sum of void volume and fiber material volume. The linear fiber density was thus 50 fibers/cm, resulting in only a 200 μm space per fiber. Panel B in Figure 1 shows a 40 μm linear fiber spacing of our artificial lungs compared to a 70 μm linear fiber spacing of commercial lungs [Fig. 1(C)]. This design speeds up device failure due to coagulation.

The test circuit was a pumpless arterio-venous (AV) shunt (Fig. 3). The inlet to outlet circuit components were each a 16 (inlet) or 14 (outlet) gauge angiocath, 1/4″ luer lock PVC connector, 3″ long 1/4″ inner diameter (ID) tygon (Fisher Scientific, Pittsburg, PA) tubing, a 1/4″–1/4″ luer lock straight polycarbonate connector, and another 3″ long 1/4″ ID tygon tubing section. The NOgen shunts were coated tip-to-tip with either the two-part silicone or with 10 wt% of 50 nm Cu(II) oxide particles (Sigma Aldrich, St. Louis, MO, Product number 544868) in tygon polymer. NOgen silicone was used to coat the angiocaths and connectors

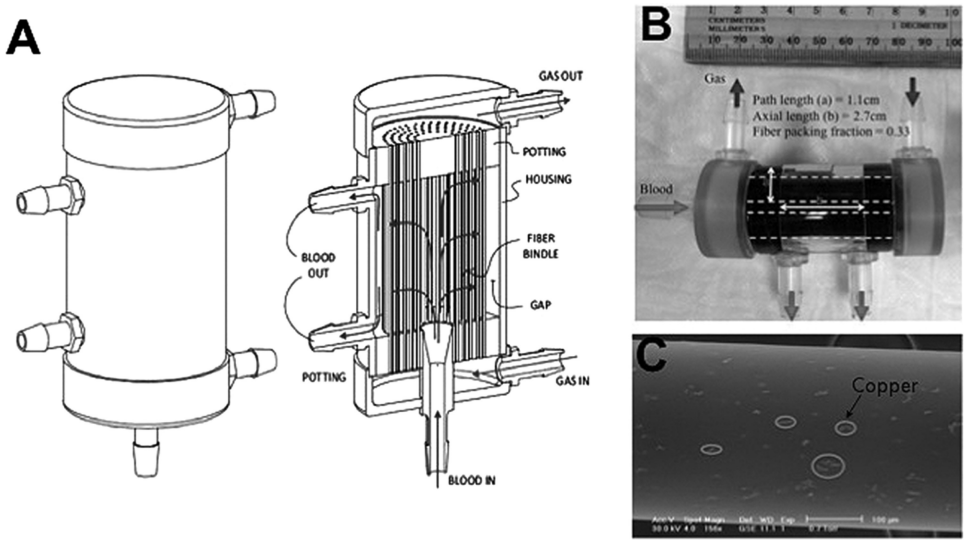

FIGURE 2. (A) Design of radial flow ECMO oxygenator (Borrowed with permission from Medarray). (B) Prototype of nitric oxide generating hollow silicone fiber oxygenator and (C) SEM (15 kV) image of NOgen silicone fiber surface showing copper catalysts. Prior to imaging, fibers were gold sputtered.

in either silicone using the synthesis procedure described previously.[19] To coat tubing, tygon pellets chopped up from tygon tubing were dissolved in tetrahydrofuran (THF; Sigma Aldrich, St. Louis, MO) using 1 g pellets per 3 mL THF by vortexing the mixture for 30 min. Cu particles were then suspended in the solution and mixed. Specifically, the Cu silicone mixture was thoroughly mixed at 2600 rpm for 30 min using a 120 V model Analog Vortex Mixer (Fisher Scientific) followed by mixing at 3500 rpm for 1 min using a DAC 150.1 FV SpeedMixer (FlackTek, SC). The resulting mixture was then coated onto the circuit tubing and cured at room temperature for 48 h.

Measurement of NO flux from fibers *in vitro*

NO generation was measured from 1 cm long tubing samples (NOgen and non-NOgen surfaces, $N = 5$ ea), and from 1 cm long fibers (NOgen and non-NOgen, $N = 5$ ea) using a Seivers nitric oxide analyzer (NOA), model 280 (Boulder, CO) according to previously described methods.[19]. In brief, *S*-nitrosoglutathione (GSNO, 1 μM), 30 mM glutathione, and 5 mM ethylenediaminetetraacetic acid, all purchased from Sigma Aldrich, were added to an amber reaction vessel containing phosphate-buffered saline (PBS, pH = 7.34) at 37°C. The solution was purged with nitrogen gas and the output gas was swept to a nitric oxide analyzer (GE Analytical Instruments, Boulder, CO) at 200 mL/min. Baseline measurements were taken for 5 min before samples were introduced into the GSNO-rich solution. The NO generated from the reaction was continuously measured, and a peak NO flux was calculated by dividing the peak NO generation rate by the sample surface area.

Rabbit thrombogenicity model for testing extracorporeal circulation (ECC) circuits

The animal handling and surgical procedures were approved by the University Committee on the Use and Care of Animals in accordance with University of Michigan and federal regulations. A total of 10 ECC circuits ($N = 5$/group) were tested for thrombogenicity using 10 adult New Zealand male rabbits (Myrtle's Rabbitry, Thompson's Station, TN). All rabbits (2.5–3.5 kg) were initially anesthetized with intramuscular injections of 5 mg/kg xylazine injectable (AnaSed Lloyd Laboratories Shenandoah, Iowa) and 30 mg/kg ketamine hydrochloride (Hospira, Lake Forest, IL). Procedures for maintenance rabbits under anesthesia, maintaining normal blood pressure, surgical procedure for placement of the AV circuit, measuring blood gases (arterial blood pH,

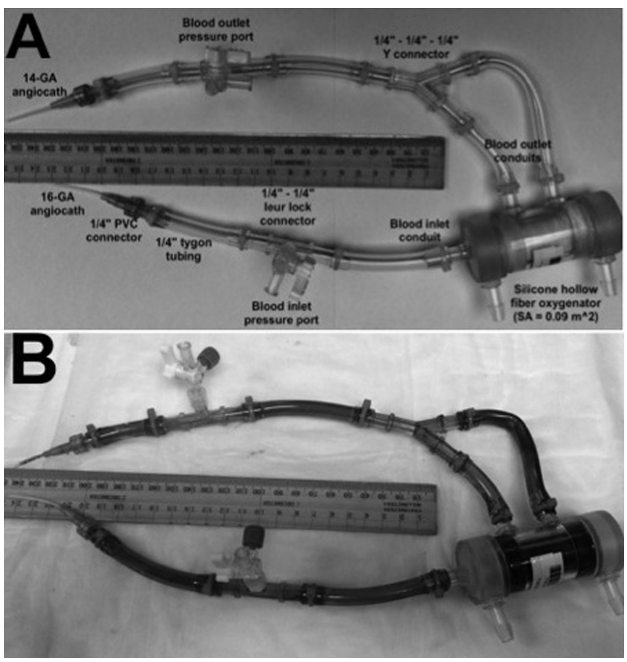

FIGURE 3. Extracorporeal circulation circuits: (A) Control (clear) and (B) NO-generating (bottom).

TABLE I. Effects of NO Generating Surface on Hemodynamic Parameters of the Extracorporeal Circulation (ECC) Circuits and Rabbits

Treatment	Parameter	Baseline[a]	Time on ECC (h) 1	2	3	4
Control ECC	MAP	39.0 ± 6.0	41.80 ± 18.80	59.50 ± 23.30	89.0 ± 45.30*	93.50 ± 43.10*
	HR	201.80 ± 30.30	208.80 ± 22.5	253.50 ± 14.80*	248.50 ± 13.40	204.0 ± 14.10
	ECC BF	63.20 ± 2.10	22.80 ± 14.0*	26.20 ± 19.40*	30.0 ± 24.40*	33.80 ± 32.80*
	ACT	331.0 ± 36.70	337.0 ± 58.0	314.5 ± 19.3	276.50 ± 18.0	307.50± 38.90
	$PaCO_2$	30.33 ± 5.80	29.60 ± 4.0	31.0 ± 0.90	30.8 0± 1.10	28.70 ± 2.54
	pH	7.48 ± 0.01	7.44 ± 0.10	7.3.0 ± 0.10	7.33 ± 0.11	7.32 ± 0.01
NOgen ECC	MAP	48.60 ± 6.20	34.40 ± 2.60*	46.80 ± 28.60	54.0 ± 16.20	52.20 ± 22.70
	HR	185.80 ± 30.40	193.60 ± 12.80	195.20 ± 17.60	194.40 ± 10.90	202.60 ± 5.10
	ECC BF	70.50 ± 6.90	83.20 ± 6.50	105.20 ± 20.40*	112.60 ± 14.40*	105.0 ± 8.70*
	ACT	362.0 ± 43.40	401.80 ± 45.60	393.20 ± 26.90	371.20 ± 20.90	376.80 ± 19.40
	$PaCO_2$	35.92 ± 5.70	35.10 ± 9.89	33.70 ± 10.07	34.76 ± 7.98	35.66 ± 6.84
	pH	7.43 ± 0.02	7.32 ± 0.11	7.31 ± 0.11	7.28 ± 0.09	7.31 ± 0.05

Values are means ± SEM.

* $p < 0.05$ versus baseline; Mixed model analysis with repeated measures.

[a] Values are just after establishing flow in ECCs. MAP = mean arterial pressure (mm Hg), HR = heart rate (beats/min), BF = blood flow (ml/min), ACT = activated clotting time (sec), $PaCO_2$ = arterial partial pressure of CO_2.

pCO_2, pO_2, total hemoglobin and methemoglobin), and measuring coagulation have all been previously published.[14,15,20] No sweep gas was employed in the fibers, as subjects were adequately supported on a Sechrist Infant Ventilator Model IV-100 (Sechrist, Anaheim, CA).

The circuit was primed with saline solution and 6 U/mL of heparin sulfate and placed into position by cannulating the left carotid artery for circuit inflow and the right external jugular vein for circuit outflow. The rabbits were given a heparin bolus (300 U/kg, IV). Activated clotting time (ACT) was measured with a hemochron blood coagulation system model 801 (International Technidyne, Edison, NJ) using 0.4 mL of blood. Once ACT was within 350–400 s, the circuit was unclamped and a 10 U/kg/h heparin infusion was initiated. In addition, 0.12 μmol/kg/min infusion of the NO donor, *S*-Nitroso-*N*-acetylpenicillamine (SNAP), was started immediately after the ECC blood flow was initiated to replace any lost NO donors in blood. Blood flow was monitored with an ultrasonic flow probe and flow meter (1/4″ ME6PXN and HT207, respectively; Transonic, Ithaca, NY). Circuit inlet and outlet pressures were measured using fluid coupled pressure transducers (Hospira, Lake Forest, IL) and a data acquisition system (Biopac Systems, Aero Camino Goleta, CA). Pressures and flow were recorded at the onset of blood flow and every 30 min thereafter. In addition, blood samples were collected every hour for measurement of blood gases, platelet and total white blood cell (WBC) counts, plasma fibrinogen concentration, activated clotting time (ACT), and platelet aggregation as performed at baseline. After 4 h, the rabbits were euthanized with Fatal Plus (130 mg/kg sodium pentobarbital; Vortech Pharmaceuticals Dearborn, MI). The circuits were then fixed in 2% glutaraldehyde and autopsied for clot inspection on their gas exchange fibers using scanning electron microscopy. To perform autopsy on the artificial lungs, their fiber bundles were excised by sectioning away the potted regions of the devices. The fiber bundles were dehydrated by bathing them with a graded series of ethanol–water mixtures from 25, 50 and 75 to 100% ethanol for 10 min each, and then dried for 30 min. Dried fibers were sputter-coated with gold, and imaged with a Hitachi S-3200N scanning electron microscope (15 kV).

Data and statistical analysis

All raw hematology data collected after baseline was corrected for hemodilution by multiplying the raw data collected at time *t* with (hemoglobin at BL/hemoglobin at time *t)*. For example, platelet count corrected for hemodilution at $t = 1$ h will be calculated as $\text{Platelet count}_{t = 1\text{ h corrected}} = (\text{hemoglobin}_{t = \text{baseline}}/\text{hemoglobin}_{t = 1\text{ h}}) \times \text{platelet count}_{t = 1\text{ h}}$. Resistance was calculated in the standard fashion as the average pressure drop across the circuit divided by the average flow rate.

All statistics were performed using SPSS (Chicago, IL). Data normality was assessed using a Shapiro–Wilk test for each dependent variable (mean arterial pressure, circuit flow, artificial lung resistance, platelet count, plasma fibrinogen, and resistance). *P*-values from the tests of normality were all greater than 0.05, indicating that the data was normally distributed. Mixed model analysis with repeated measures was then used to determine the effect of circuit type (NOgen or control) on each dependent variable. Experimental time was used as the independent, repeated variable, and the experiment number was the subject variable. In each case, the baseline data points were excluded as this data is taken prior to application of the treatment (NOgen or control). Finally, alternative covariance structures were compared using information criteria (e.g., AIC, BIC). In all cases, a Toeplitz covariance structure was found to have the best fit. In addition, a similar mixed model was performed to determine if each independent variable varied significantly from baseline, using the following exceptions: (1) the NOgen and control data was analyzed separately, (2) the baseline data was included, and (3) a Bonferroni correction was used when comparing each time to baseline. A *p*-value

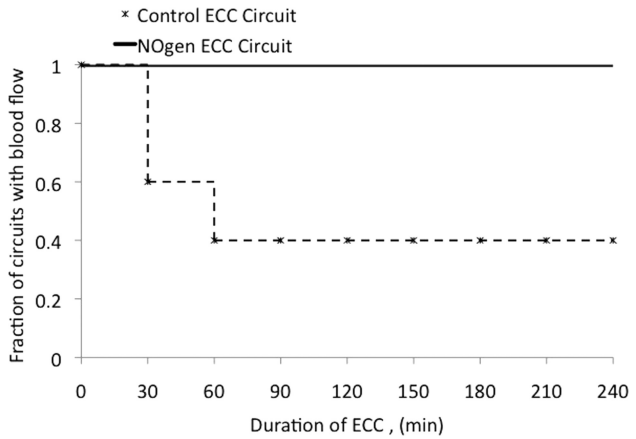

FIGURE 4. Survival of control and experimental ECC circuits after flow initiation.

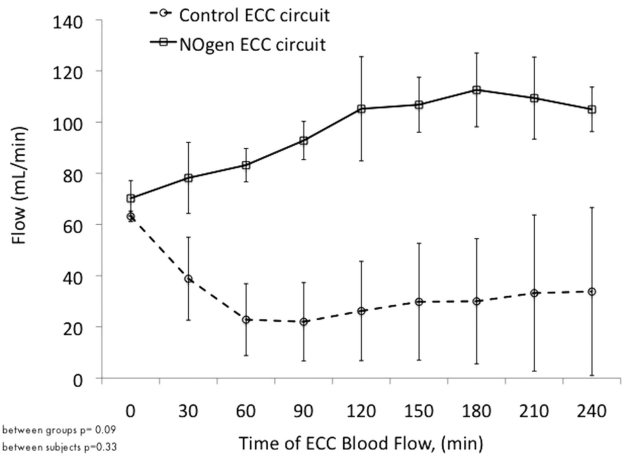

FIGURE 5. Time course blood flow in control and NOgen ECC circuits.

< 0.05 is regarded as significant. Kaplan–Meier analysis was used to estimate the survival of circuit type, and statistical differences in all baseline data between circuit types were analyzed using a student *t*-test.

RESULTS

In vitro NO flux from fibers

The NO flux from fibers and tubing containing 10 wt% Cu particle (50 nm) were $12 \pm 4 \times 10^{-10}$ mol/cm^2/min and $14.7 \pm 2.5 \times 10^{-10}$ mol/cm^2/min, respectively. Addition of the control fibers and circuits to the NO donor media resulted in no additional NO release over baseline readings.

General rabbit physiology

Table I presents general rabbit physiology in each group. Baseline data on PaO_2, pH, and mean arterial pressure (MAP) were significantly different between circuit types at $p = (0.01, 0.008, 0.04)$, respectively. Baseline data were taken minutes after initiating blood flow. In Table I, baseline MAP in both NOgen and control groups were lower than normal rabbit MAP. In addition, baseline data on blood flow, $PaCO_2$, and heart rate were not different between circuit group at $p = (0.28, 0.58, \text{and } 0.42)$, respectively. Over the course of the study, heart rate and MAP were significantly higher in the control group (223.0 ± 25.6 bpm, 64.5 ± 25.0 mmHg) than in the NOgen group (194.7 ± 6.1 bpm, 42.7 ± 7.7 mmHg; $p < 0.05$) due to the vasodilatory effect of NO on blood vessels. Partial pressures of CO_2, O_2, and pH were relatively normal and stable in the control (30.1 ± 2.9 mmHg, 125.8 ± 3.1 mmHg, 7.39 ± 0.05) and NOgen (35.0 ± 8.10 mmHg, 289.8 ± 15.2 mmHg, 7.33 ± 0.08) groups. There was minor acidosis in the NOgen group, which may be due to greater AV shunt flow and resultant reduced peripheral perfusion (see below).

ECC blood flow and artificial lung resistance

The Kaplan–Meier survival for flow in control and NOgen circuits is shown in Figure 4. All NOgen circuits remained patent for the entire test duration. In contrast, two control circuits had no blood flow after 30 min and one more had none after 60 min. For the remaining controls, one maintained at least baseline flows while the other had flows significantly less than baseline levels ($p < 0.01$). On the other hand, blood flow increased from baseline levels almost approaching significance ($p = 0.07$; Fig. 5) in the NOgen group. This may be due to a combination of no significant change in resistance (see below) and the increase in mean arterial pressure that occurs over the course of the experiment. Blood flow through these circuits is driven by the pressure gradient between the artery and vein. Initiation of blood flow led to arterial hypotension volume shifts and likely an inflammatory response to the artificial circuits. The hypotension then lessened over the course of the experiment. This may have been due to a compensatory increase in cardiac output, but this data was not taken. Ultimately, as the arterial pressure increased, ECC flow also increased in the relatively clot-free NOgen groups, but the increment was small and not significantly different from baseline flow.

The decrease in flow in the control group was due to an increase in resistance due to thrombus formation. The resistance in the NOgen circuits (dark bars) and control

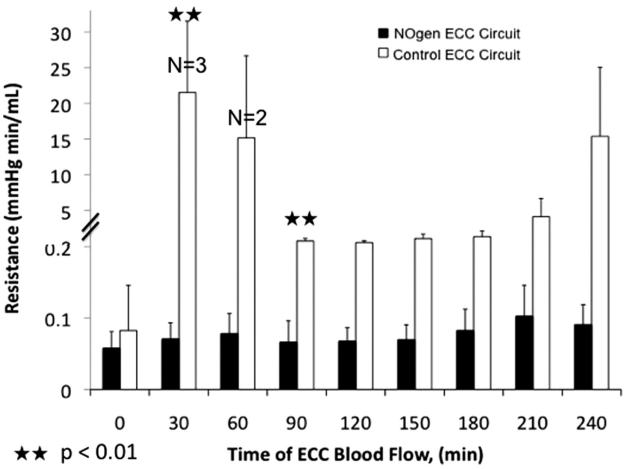

FIGURE 6. Time course blood flow resistance in control and NOgen ECC circuits.

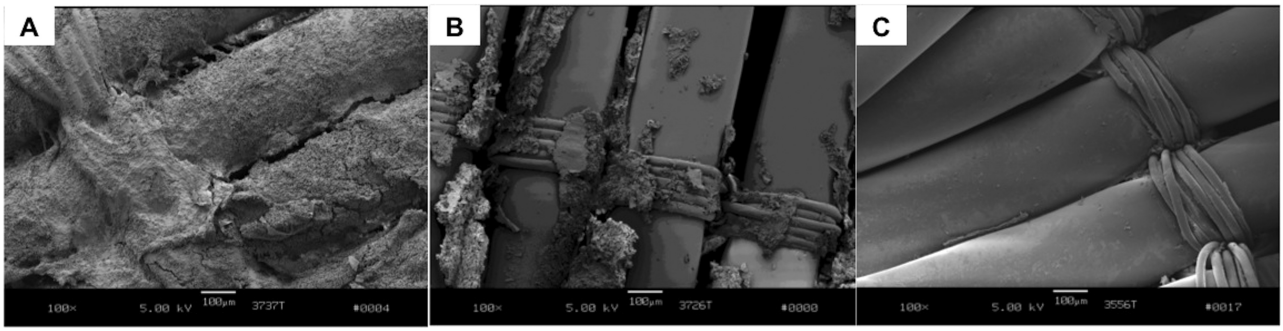

FIGURE 7. Scanning electron micrographs of the artificial lung fibers showing clot formation on the outer layers of fibers from (A) a failed control lung, (B) a control lung that survived 4 h, and (C) a NOgen lung.

circuits (clear bars) is shown in Figure 6. Resistance did not change significantly with time in the NOgen group ($p < 0.01$). In the control group, all resistances from 30 to 240 min were significantly higher than baseline resistance ($p < 0.01$). Resistance in the control group raised from 0.08 ± 0.06 mmHg min/mL at baseline to 21 ± 9 mmHg min/mL at 30 min. Thereafter, devices with infinite resistance (zero blood flow) were removed from the data as they failed, but resistance values remained over 5.5 ± 2.5 mmHg min/mL for the two devices that retained some blood flow. Autopsy results from control and NOgen lungs, shown in Figures 7 (gross, fiber level view) and 8 (fine, surface topography), revealed significantly less clot formation on the NOgen lungs' gas exchange fibers compared to controls. It can be seen quite starkly that clot formation on the control lungs led to their increased resistance to blood flow, decreased flow, and failure. Moreover, as expected, it can be seen that clot formation is more severe in control devices that failed than in those that did not fail.

Hematology

Activated clotting times were generally higher in NOgen than in control group. At baseline, ACT in NOgen (362.0 ± 97.2 s) was not significantly higher than control (385.8 ± 82.3, $p = 0.68$). It also did not increase or decrease significantly after 4 h of blood flow in NOgen (376.5 ± 86.9, $p = 0.76$) and control (307.5 ± 86.9, $p = 0.3$) groups, respectively. Methemoglobin levels remained below 0.9 ± 0.3% of total hemoglobin in all circuits. In both control and NOgen groups, platelet counts dropped significantly ($p < 0.05$) to 58.3 ± 5.6% and 53.5 ± 4.3% of baseline counts, respectively, after an hour of extracorporeal circulation (ECC; Fig. 9). In addition, the duration of blood flow had an effect on platelet count ($p < 0.01$) but not plasma fibrinogen ($p = 0.21$). Between hour 1 and 4, platelet counts and plasma fibrinogen did not change in control group now of size $N = 2$, whereas only platelet count was significantly lower at hour 4 in NOgen group ($p < 0.05$) compared to hour 1 (Fig. 9). White blood cell counts (Fig. 10) were significantly higher in the controls circuits ($p < 0.05$). White blood counts significantly increased from baseline ($p < 0.05$), peaking at 200% of baseline after 2 h of blood flow in controls. In the NOgen group, a slight and insignificant ($p = 0.14$) rise in WBC was observed at 1 h and thereafter returned to baseline values.

Plasma copper concentration

Serum copper level at the onset of blood flow in control group (132.8 ± 4.5 µg/dL) was not significantly different from the NOgen group (134.7 ± 22.5 µg/dL, $p < 0.01$). As expected, baseline copper level was maintained for 4 h in the control group ($p < 0.01$). However, plasma copper levels

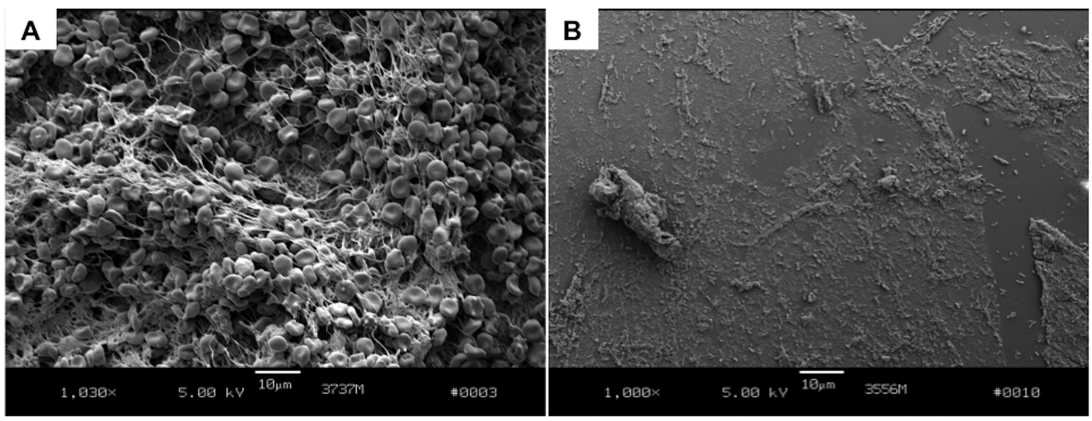

FIGURE 8. Scanning electron micrographs of the artificial lung fiber surfaces of (A) control and (B) NOgen fibers taken from fiber layers in the middle of the device. Control surfaces contain far more platelet deposition than NOgen surfaces.

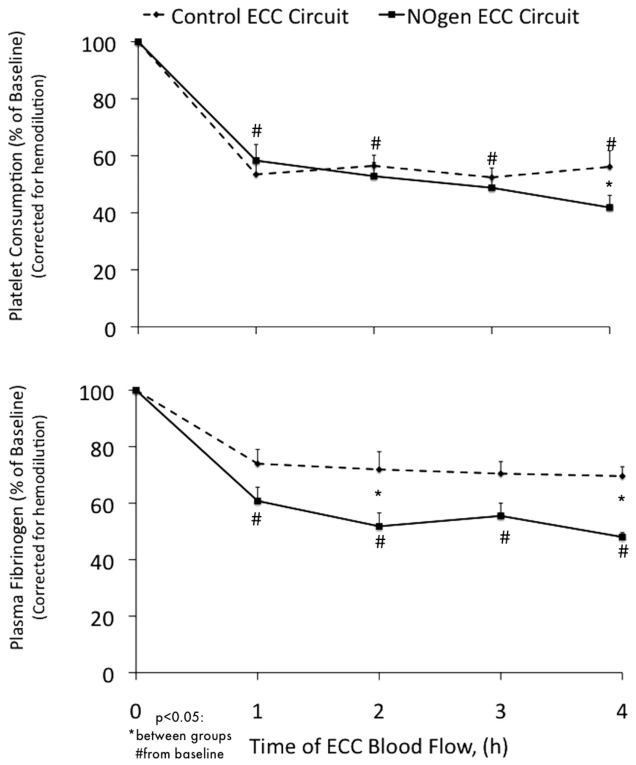

FIGURE 9. Levels of platelet consumption and plasma fibrinogen concentration during extracorporeal circulation.

in the NOgen group significantly increased to 2.8 times baseline levels ($p < 0.001$).

DISCUSSION

The aim of this study was to develop a copper-mediated, NO generating, hollow fiber membrane lung, and evaluate its thrombogenicity. These fibers were created successfully and capable of $12 \pm 4 \times 10^{-10}$ mol/cm^2/min of NO flux. It should be noted that NO flux is calculated in the traditional way as moles of NO release per unit time per unit area. Therefore, as the same amount of Cu (10 wt% of Cu/polymer matrix) was added to fibers and to tubing, both surfaces had similar catalytic activity on NO donors and thus similar rate of NO release per unit area. Previous 10 wt% surfaces with either 3 μm[19] and 50 nm[21] copper particles produced 9×10^{-10} and 15×10^{-10} mol/cm^2/min, respectively, under identical *in vitro* conditions. Due to the NO flux, the NOgen ECC lungs were less thrombogenic than their non-NOgen controls. The NO generating ECC lungs showed markedly less surface clot formation and were thus all patent for the duration of the study. In contrast, 60% of the control lungs clotted off enough to completely eliminate blood flow after an hour of circulation.

It should be noted that the artificial lung fiber bundle design presents an exceedingly challenging test for evaluating biocompatibility. As discussed earlier, the fiber bundles were packed very densely to maximize artificial surface and hasten coagulation. There is only an average of 40 μm between adjacent fibers and, moreover, adjacent fiber layers are directly touching with no space between them. Thus, even a small amount of thrombus can markedly occlude the blood flow path. In the NO lungs, platelet binding appears to be largely eliminated, keeping these narrow channels open.

Despite these positive results, systemic platelet counts did not differ between the NOgen and control groups. For this to be true, all experiments must have resulted in the same loss of platelets. Yet, SEMs indicate very little platelet binding to the NOgen lungs and significant binding on the control lungs. Several issues might explain this paradox. First, only two control devices remained patent at 1 h. Thus, the low survival rate in the control group means that platelet consumption data for the control group shown in Figure 9 is largely representative of the two surviving control devices. These devices had a lesser amount of clot formation and platelet binding. Second, it is our hypothesis that NO reduced platelet binding to the lungs but did not fully eliminate platelet activation in flowing blood due to surface-generated, pro-coagulant molecules such as thrombin. In this scenario, platelets would continue to pass through the lung but would then be removed in the rabbit by the mononuclear phagocyte system.[22,23]. The hypothesis of surface-generated thrombin, which induces activation of circulating platelets, is supported by the fact that plasma proteins of the contact system of the coagulation cascade can still adsorb to prosthetic surfaces even in the presence of NO.[16,24] Adsorption of contact system proteins such as FXII and kallikrein lead to thrombin generation in plasma, which in turn activates flowing platelets.[16,25]

To that point, fibrinogen adsorption was larger in the NO-generating group than in controls. Greater fibrinogen adsorption has been observed in previous blood studies where copper particles were coated onto circuit tubing.[15] This effect could be due to a rougher NOgen surface or due to charge interaction between the polymer surface, where an oxidation–reduction reaction is constantly taking place, and the polar terminals of plasma fibrinogen. The mechanisms of interaction among the NOgen surface, NO

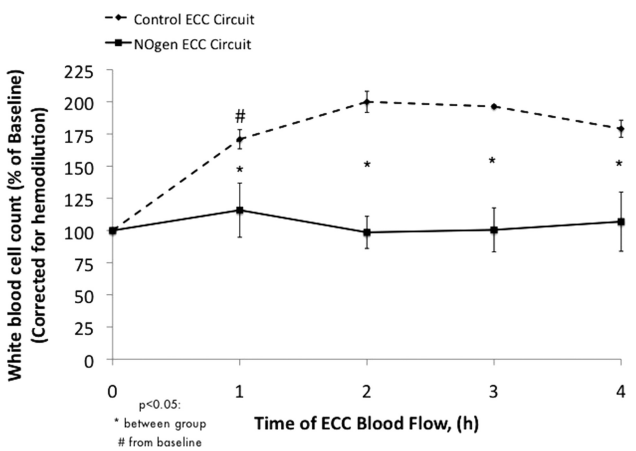

FIGURE 10. Time course white blood cell counts in control and NOgen ECC circuit groups.

generation and fibrinogen activation is, however, still not clear.[14,26,27] Future studies, therefore, should examine protein adsorption and activation at the surface in more detail and seek to reduce it. To reduce it, surface coatings could be employed that create a smoother and less adsorptive surface. This top-coat must be thin, however, such that it does not significantly inhibit hydration, corrosion, and ionization of copper at the blood/polymer interface.

Circuits with NO flux also maintained baseline white blood cell counts, whereas control circuits caused a significant increase. Further studies are necessary to determine the cause in these devices, but previous research suggests a possible mechanism. Activated platelets are known to release chemokines, including RANTES, platelet factor 4, and epithelial neutrophil-activating protein 78.[28,29] If this is occurring in this study, it may draw monocytes to the surface and further accelerate clot formation and systemic inflammation. Platelet P-selectin binds monocytes first via their P-selectin glycoprotein (PSGL-1) and, afterwards, form firmer bonds between monocyte CD11b/CD18 and platelet GPIbα directly and GpIIb/IIIa indirectly using fibrinogen as a bridging molecule.[28,30] This, in turn, activates the monocyte, causing it to release both pro-coagulant and pro-inflammatory molecules. Major *et al.*[24] demonstrated that NO flux from tubing in extracorporeal circuits decreased monocyte activation, as demonstrated by CD11b expression. It is also possible that NO has a more direct effect on white cells but this has not yet been demonstrated.

The main disadvantage of NOgen is leaching of copper into blood. Although copper is an essential trace element present in normal diet, excess of it in serum can be toxic. Potential adverse effects of copper toxicity include irritation of the eyes, mouth, and nose, nausea, liver and kidney failure, and even loss of life after a high intake. According to the food and drug administration (FDA), about 2 mg of copper per day is required by the average adult with an acceptable daily intake of 0.5 mg per kg body weight. Thus, the acceptable daily total Cu intake could be 37 mg for a 75 kg man with 5 L total blood volume. If absorbed all at once, this would lead to a blood copper concentration of 750 μg/dL. The amount of copper in the blood was 333 ± 3.9 μg/dL after 4 h but does not include any copper diffusing into tissues. It is unclear if this level would lead to toxic effects.

Ultimately, further, long-term studies are required to examine device biocompatibility. This includes coagulation, inflammation, copper leaching, and their effect on organ function over a period of weeks. If copper leaching leads to toxicity, this will limit the clinical applicability of this approach to short-term procedures such as cardiopulmonary bypass, dialysis, and to small surface area devices such as catheters, vascular grafts, patches, and stents. If this is proven to be a problem, alternate or mixed catalysts such as organoselenium could be explored.[31]

CONCLUSION

This study evaluated the first Cu-mediated NO-generating hollow silicone fiber lung in an ECC setup. The results indicate that NO-generating hollow fiber lungs significantly reduce blood coagulation compared to their non-NO-generating controls. The resistance of the NO generating artificial lungs did not change significantly over the course of 4 h, while the 60% of the control lungs occluded completely. Accordingly, the control group had significant lower blood flow and significantly higher resistance due to occlusive clot formation.

REFERENCES

1. Conrad SA, Zwischenberger JB, Grier LR, Alpard SK, Bidani A. Total extracorporeal arteriovenous carbon dioxide removal in acute respiratory failure: A phase I clinical study. Intensive Care Med 2001; 27:1340–1351.
2. Vaslef SN. Implantable artificial lungs: Fantasy or feasibility. Landes Biosci 2001; 116–126,.
3. Zwischenberger JB, Conrad SA, Alpard SK, Grier LR, Bidani A. Percutaneous extracorporeal arteriovenous CO2 removal for severe respiratory failure. Ann Thorac Surg 1999;68:181–187.
4. Wang D, Lick SD, Zhou X, Liu X, Benkowski RJ, Zwischenberger JB. Ambulatory oxygenator right ventricular assist device for total right heart and respiratory support. Ann Thorac Surg 2007; 84: 1699–1703.
5. Larson DF, Arzouman D, Kleinert L, Patula V, Williams S. Comparison of Sarns 3M heparin bonded to Duraflo II and control circuits in a porcine model: Macro- and microanalysis of thrombi accumulation in circuit arterial filters. Perfusion 2000;15:13–20.
6. Larm O, Larsson R, Olsson P. A new non-thrombogenic surface prepared by selective covalent binding of heparin via a modified reducing terminal residue. Biomater Med Devices Artif Organs 1983;11:161–173.
7. Tayama E, Hayashida N, Akasu K, Kosuga T, Fukunaga S, Akashi H, Kawara T, Aoyagi S. Biocompatibility of heparin-coated extracorporeal bypass circuits: New heparin bonded bioline system. Artif Organs 2000;24:618–623.
8. Engbers GH, Feijen J. Current techniques to improve the blood compatibility of biomaterial surfaces. Int J Artif Organs 1991;14: 199–205.
9. Palanzo DA, Zarro DL, Manley NJ, Montesano RM, Quinn M, Elmore BA, Gustafson PA, Castagna JM. Effect of Carmeda-BioActive surface coating versus TrilliumTM biopassive surface coating bypass coating of the oxygenator on circulating platelet count drop during cardiopulmonary bypass. Perfusion2001;16:279–283.
10. Kim WS, Jacobs H. Design of nonthrombogenic polymer surfaces for blood-contacting medical devices. Blood Purif 1996; 14: 357–372.
11. Do YS, Kao EY, Ganaha F, Minamiguchi H, Sugimoto K, Lee J, Elkins CJ, Amabile PG, Kuo, Wang DS, Waugh JM, Dake. In-stent restenosis limitation with stent-based controlled-release nitric oxide: Initial results in rabbits. Radiology 2004; 230:377–382.
12. Palmer RM, Ferrige AG, Moncada S. Nitric oxide release accounts for the biological activity of endothelium-derived relaxing factor. Nature 1987;337:524–526.
13. Kolpakov V, Gordon D, Kulik TJ Nitric oxide-generating compounds inhibit total protein and collagen synthesis in cultured vascular smooth muscle cells. Circ Res 1995;76:305–309.
14. Major TC, Brant DO, Reynolds MM, Bartlett RH, Meyerhoff ME, Handa H, Annich GM. The attenuation of platelet and monocyte activation in a rabbit model of extracorporeal circulation by a nitric oxide releasing polymer. Biomaterials 2010;31:2736–2745.
15. Major TC, Brant DO, Burney CP, Amoako KA, Annich GM, Meyerhoff ME, Handa H, Bartlett RH. The hemocompatibility of a nitric oxide generating polymer that catalyzes S-nitrosothiol decomposition in an extracorporeal circulation model. Biomaterials 2011;32:5957–5969.
16. Colman RW, Hirsh J, Marder VJ, Clowes AW, George NJ. Hemostasis and Thrombosis: Basic Principles & Clinical Practice, 4th ed. Philadelphia, PA: Lippincott Williams & Wilkins, ; 2001.
17. Wu Y, Rojas AP, Grifth GW, Skrzypchak AM, Lafayette N, Bartlett RH, Meyerhoff ME. Improving blood compatibility of intravascular oxygen sensors via catalytic decomposition of S-nitrosothiols to generate nitric oxide in situ. Sens Actuators B Chemi 2007;121: 36–46.

18. Oh BK, Meyerhoff ME. Catalytic generation of nitric oxide from nitrite at the interface of polymeric films doped with lipophilic Cu(II)-complex: A potential route to the preparation of thromboresistant coatings. Biomaterials 2004;25:283–293.
19. Amoako KA, Cook KE. Nitric oxide-generating silicone as a blood-contacting biomaterial. ASAIO J 2012;58:539–544.
20. Amoako KA, Archangeli C, Major TC, Meyerhoff ME, Annich GM, Bartlett RH. Thromboresistance characterization of extruded nitric oxide releasing silicone catheters. ASAIO J 2012;58:238–246.
21. Amoako KA. Nitric oxide therapies for local inhibition of platelets' activation on blood-contacting surfaces. PhD Dissertation, University of Michigan; 2012.
22. Maugeri N, Rovere-Querini R, Evangelista V, Covino C, Capobianco A, Bertilaccio MTS, Piccoli A, Totani L, Cianflone D, Maseri A, Manfredi AA. Neutrophils phagocytose activated platelets in vivo: A phosphatidylserine, P-selectin, and integrin-dependent cell clearance program. Blood 2009; 113:5254–5265.
23. Fufa D, Shealy B, Jacobson M, Kevy S, Murray M. Activation of platelet-rich plasma using soluble type I collagen. J Oral Maxillofac Surg 2008;66:684–690.
24. Tevaearai HT, Mueller XM, Tepic S, Cotting J, Boone Y, Montavon PM, Von Segesser LK. Nitric oxide added to the sweep gas infusion reduces local clotting formation in adult blood oxygenators. ASAIO J 2000;46:719–722.
25. Kwaan HC, Walter Bowie EJ. Thrombosis. Philadelphia, PA: W.B. Saunders Company; 1982.
26. Grunkemeier JM, Tsai WB, McFarland CD, Horbett TA. The effect of adsorbed fibrinogen, fibronectin, von Willebrand factor and vitronectin on the procoagulant state of adherent platelets. Biomaterials 2000;21:2243–2252.
27. Wu Y, Zhou Z, Meyerhoff ME. In vitro platelet adhesion on polymeric surfaces with varying fluxes of continuous nitric oxide release. J Biomed Mater Res Part A 2007; 81:956–963.
28. Gawaz M, Langer H, May AE. Platelets in inflammation and atherogenesis. JClin Invest 2005;115:3378–3384.
29. Weber C. Platelets and chemokines in atherosclerosis: Partners in crime. Circ Res 2005;96:612–616.
30. Furie B, Furie BC. The molecular basis of platelet and endothelial cell interaction with neutrophils and monocytes: Role of P-selectin and the P-selectin ligand, PSGL-1. Thromb Haemost 1995;74: 224–227.
31. Cha W, Meyerhoff ME. Catalytic generation of nitric oxide from S-nitrosothiols using immobilized organoselenium species. Biomaterials 2007;28:19–27.